Casimir effect in active matter systems

D. Ray,[1,2] C. Reichhardt,[1] and C. J. Olson Reichhardt[1]
[1]*Theoretical Division, Los Alamos National Laboratory, Los Alamos, New Mexico 87545, USA*
[2]*Department of Physics, University of Notre Dame, Notre Dame, Indiana 46556, USA*
(Received 11 March 2014; published 23 July 2014)

We numerically examine run-and-tumble active matter particles in Casimir geometries composed of two finite parallel walls. We find that there is an attractive force between the two walls of a magnitude that increases with increasing run length. The attraction exhibits an unusual exponential dependence on the wall separation, and it arises due to a depletion of swimmers in the region between the walls by a combination of the motion of the particles along the walls and a geometric shadowing effect. This attraction is robust as long as the wall length is comparable to or smaller than the swimmer run length, and is only slightly reduced by the inclusion of steric interactions between swimmers. We also examine other geometries and find regimes in which there is a crossover from attraction to repulsion between the walls as a function of wall separation and wall length.

DOI: 10.1103/PhysRevE.90.013019 PACS number(s): 47.63.Gd, 82.70.Dd, 64.75.Xc, 87.18.Hf

I. INTRODUCTION

The Casimir geometry consists of two finite parallel plates placed at a fixed distance from each other that experience an attraction due to the confinement of fluctuations in the media between the plates [1]. In the original Casimir effect calculation, electromagnetic vacuum fluctuations produce an attractive force between two metal places in a vacuum. Much later, Casimir forces were experimentally measured [2], and they have recently been studied in a variety of systems in order to understand how to control their magnitude [3] or polarity [4]. Confined classical fluctuations can produce the so-called critical Casimir effect [5–7], first proposed by Fisher and de Gennes near critical demixing in bulk mixtures. The critical Casimir effect has been directly measured [8] and studied in various colloidal systems where it can produce colloidal aggregation [8–10]. Casimir type effects have also been studied in granular media, where attractive forces arise between objects or plates placed in vibrated or flowing sand [11]. Critical Casimir effects have also been proposed to occur near percolation thresholds [12] and in biological systems such as near fluctuating cellular membranes [13]. The ability to enhance or control such forces can lead to a wide variety of applications in self-assembly, particle transport, and the creation of novel devices.

Strong fluctuations appear in active matter or self-driven particle systems [14] such as swimming bacteria undergoing run-and-tumble dynamics [15,16]. Recently a number of nonbiological active matter systems have been realized experimentally, including artificial swimmers [17], self-driven colloids [18–20], or light-activated colloidal particles performing a directed random walk [19–21]. Particles undergoing run-and-tumble dynamics or active Brownian motion can phase separate at large run length or high density, forming dense regions separated by a dilute active gas [21–24]. Monodisperse active particles, such as self-propelled disks, can form intermittent dense patches with crystalline order, termed "living crystals" [20]. It has been shown that run-and-tumble dynamics and active Brownian motion can be mapped onto each other when the motility parameters depend on the particle density, so that results obtained with one class of system should be generalizable to the other [25].

Here we demonstrate that a Casimir-like attractive force arises between two plates placed in a bath of active particles and can be controlled by changing the plate geometry. There is already some evidence that active matter can induce forces on objects. One example is the ratchet effect observed for swimming bacteria and run-and-tumble particles in an array of asymmetric funnels in dilute or semidense regimes [16,26–29]. Here, when the active particles run along the funnel walls they can escape through the easy direction of the funnel or become trapped in a funnel tip. Their continued swimming produces forces on the funnel walls they contact. Such induced forces were more clearly demonstrated in systems where an untethered asymmetric sawtooth gear rotates in a preferred direction when placed in a bacterial bath [30,31], but only if the bacteria are actively swimming. In simulations, asymmetric objects placed in an active matter bath are pushed to produce an active matter-driven micro-shuttle [32,33].

In the Casimir geometry, there are no sharp corners in which the particles can accumulate [34]; however, we show that confinement effects alone are sufficient to create fluctuation-induced forces. The magnitude of the attractive force increases with increasing run length and can vary over several orders of magnitude. For fixed run length, the force F between the plates as a function of plate spacing d obeys $F(d) \propto \exp(-d/\lambda)$, rather than a power law which is usually observed in Casimir geometries [1,2,4,6]. The attractive force arises due to the depletion of the particle density between the plates by a combination of the motion of the particles along the walls and geometric shadowing, both of which increase with increasing run length. It is *not* an excluded volume effect or depletion interaction of the types studied in Refs. [10,35,36], since in our model the particles and walls are of vanishing width. We also examine other geometries and show that it is possible to control the magnitude of the forces and induce a crossover from an attractive to a repulsive force. For the case of infinite walls, we analytically derive the force as a function of the distance between the walls.

II. SIMULATION

In Fig. 1 we show a schematic of our system which resides in a two-dimensional (2D) simulation box of size $L_x \times L_y$ with

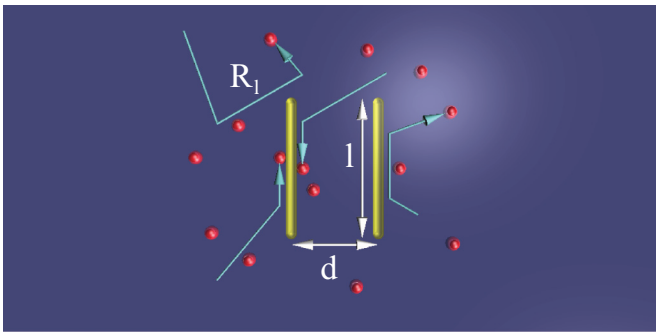

FIG. 1. (Color online) A schematic of the system containing run-and-tumble particles (balls) with some particle trajectories indicated by lines and arrows. The run length is R_l. The two parallel walls (bars) of length l are separated by a distance d. When a particle moves along a wall it imparts a force against the wall. We measure the net force per particle $\Delta F/N = (|F_{\rm out}| - |F_{\rm in}|)/N$.

periodic boundary conditions in the x and y directions. Unless otherwise noted, we take $L_x = 120$ and $L_y = 60$. Within the box are N active particles and two parallel walls of length l separated by a distance d. The run-and-tumble particles move in a fixed randomly chosen direction during a running time τ before undergoing a tumbling event and running in a new randomly chosen direction. Since we consider the dilute limit where particle-particle interactions are rare, for efficiency we use event-driven (ED) dynamics simulations and neglect particle-particle interactions. The particles run with speed $v = 1$ and travel a run length of $R_l = \tau v$ between tumbles. A particle contacting a wall at an angle θ moves with velocity $\sin\theta$ along the wall and exerts a force $\cos\theta$ on the wall. A particle that reaches the end of the wall before tumbling resumes its original swimming direction. The assumption that run-and-tumble particles move along or accumulate at walls was confirmed in ratchet geometry [16] and asymmetric gear experiments [30,31] and observed in simulations [26–28]. We measure the time-averaged forces $F_{\rm out}$ ($F_{\rm in}$) imparted on the outer (inner) surfaces of the walls. The net force per particle acting to bring the walls together or apart is $\Delta F/N = (|F_{\rm out}| - |F_{\rm in}|)/N$. We confirm our results using molecular dynamics (MD) simulations with and without particle-particle interactions [26], where we implement the steric interactions via a short-range harmonic repulsion between the particles which have a radius of $r_d = 0.25$. We find that all of our results are robust for the particle densities we consider.

III. RESULTS

A. Attractive force on walls

In Fig. 2(a) we plot the normalized force $\Delta F/N$ versus d for ED simulations of a system with $l = 20$ at various run lengths. $\Delta F/N$ increases with increasing R_l, and we find $\Delta F(d) \propto A\exp(-d/\lambda)$, with λ increasing for increasing R_l. At small run lengths such as $R_l = 1$, $\Delta F/N$ becomes very small, and in the Brownian limit of infinitesimal R_l, $\Delta F/N = 0$. In Fig. 2(b) we plot ΔF versus R_l for the same system at various d, showing that the attractive force increases with increasing R_l and saturates at large R_l.

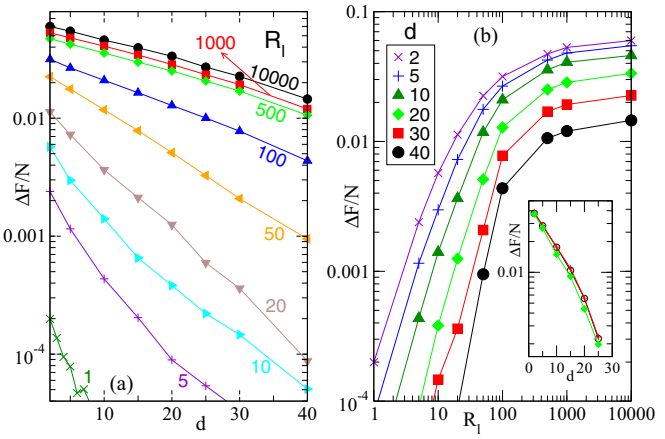

FIG. 2. (Color online) (a) $\Delta F/N$, the attractive force between the walls, vs d, the interwall distance, from ED simulations with $l = 20$, for various R_l, showing an exponential behavior. (b) $\Delta F/N$ vs R_l for the same system at various d. For large R_l, $\Delta F/N$ saturates. Inset: $\Delta F/N$ vs d for $l = 20$, $R_l = 40$, and $N = 400$ in ED simulations (•) and MD simulations without (+) and with (♦) steric particle-particle interactions.

To verify the robustness of the results, we perform three different types of simulations highlighted in the inset of Fig. 2(b) where we plot $\Delta F/N$ vs d for systems with $N = 400, l = 20$, and $R_l = 40$. We find nearly identical results for ED simulations and MD simulations with and without steric interactions, indicating that our results are robust for interacting particles in the dilute limit. We expect that at higher densities, phase separation or clustering will become important if steric particle-particle interactions are included [22–24].

In order to better understand the origin of the attractive force, in Fig. 3 we plot $\rho_v(\mathbf{r})$, the rate at which individual

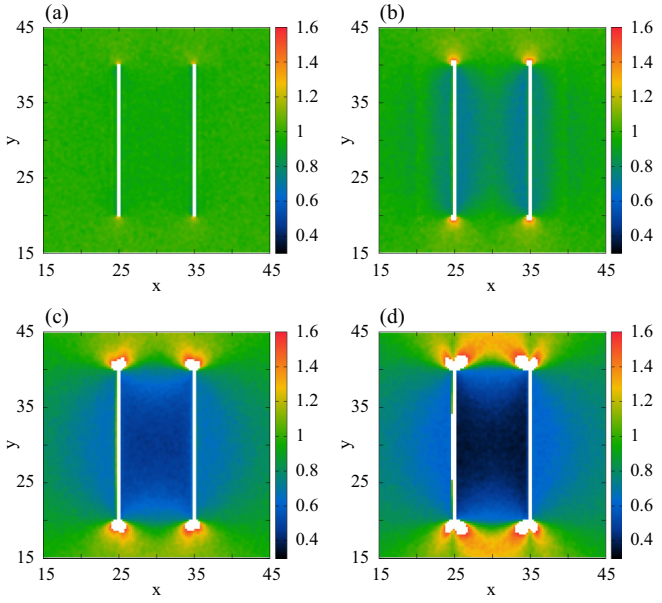

FIG. 3. (Color online) $\rho_v(\mathbf{r})$, the rate at which locations are visited by particles, for the system in Fig. 2(a) with $L_x = 60, l = 20$, and $d = 10$ at $R_l = 1$ (a), 5 (b), 20 (c), and 50 (d). ρ_v between the plates drops with increasing R_l, giving a larger attractive force.

spatial locations are visited by particles, from ED simulations with $L_x = 60$, $l = 20$, and $d = 10$ for different values of R_l. We use the normalization that $\rho_v = 1.0$ in a homogeneous system without walls. In Fig. 3(a), for short run lengths $R_l = 1$, $\rho_v \approx 1$ everywhere and $\Delta F/N \approx 0$. At larger R_l in Figs. 3(b) and 3(c), two trends appear. First, particles near the walls strike the walls and run along them rather than being reflected, raising ρ_v along the wall surfaces and diminishing ρ_v nearby; since these particles increasingly reach the end of the wall before tumbling as R_l/l increases, the regions at the ends of the walls are traversed very frequently by particles, forming spots of high ρ_v. Secondly, a geometric shadowing effect depresses ρ_v in the inner region between the walls. This region can only be replenished by bulk particles that enter the narrow gap between walls. This will occur with diminishing frequency as the gap size d decreases. In contrast, the region just outside the walls is replenished from the bulk, whose population is continually refreshed by particles reaching the end of either side of a wall. Since the inner and outer wall surfaces are populated by particles arriving from the inner and outer regions respectively, an imbalance occurs with more particles accumulating on the outer wall surfaces than the inner surfaces. The result is a nonzero $\Delta F/N$ which increases as R_l is increased or d is decreased. For very long $R_l = 50$ in Fig. 3(d), additional features appear in ρ_v at the wall ends due to the periodic boundary conditions.

These results show that Casimir attractive forces can arise in active matter systems and that they can be controlled by modifying the run length of the swimming particles. The Casimir effect that we observe is not a critical Casimir effect since we are not at a critical point. Instead, the fluctuations or straight runs of the run-and-tumble particles are cut off by the walls, producing a relative drop in the number of particles on the inner walls.

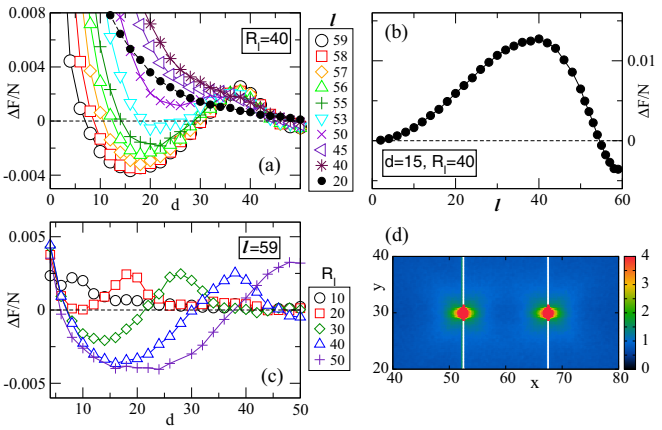

FIG. 4. (Color online) (a) $\Delta F/N$ vs d for a system with $R_l = 40$ and various l. Negative forces appear when l approaches L_y. (b) $\Delta F/N$ vs l for fixed $d = 15$ and $R_l = 40$. (c) $\Delta F/N$ vs d for a system with $l = 59$ at various R_l. (d) $\rho_v(\mathbf{r})$ for a system with $l = 58$, $d = 15$, and $R_l = 40$, in the negative force regime.

B. Reverse Casimir effect

We next consider the effect of increasing l, the wall length. Since we have periodic boundary conditions, when l approaches L_y the system is better described as having apertures of width $w = L_y - l = 60 - l$, as shown in Fig. 4(d) for a system with $w = 2$. In Fig. 4(a) we plot $\Delta F/N$ versus d for increasing l, showing that for $l \geqslant 53$, $\Delta F/N$ becomes negative over a range of d, while at larger d it becomes positive again. The magnitude of the negative force depends on l, and is largest for the smallest aperture sizes, as shown in Fig. 4(b). Here $\Delta F/N$ is nearly zero at small l and increases with increasing l up to $l \approx 40$ due to the shadowing effect. For $l > 40$, $\Delta F/N$ decreases rapidly and becomes negative due to a particle trapping effect that occurs as the system enters the aperture limit. The particles moving along an outside wall return to the bulk upon reaching the wall end when l is small, but for large l they instead are trapped by the interior region, raising the interior density and producing a net repulsive force. This trapping effect becomes more prominent with decreasing w. In Fig. 4(a) regarding the curves with $l \geqslant 53$ where negative forces can occur, for $d < 30$ the particles in the interior region spend most of their time running along the interior walls, producing a repulsive force. For $d > 30$ the particles have a chance to turn away from the inside wall during their run and avoid striking it, so the force becomes attractive again.

In Fig. 4(c) we plot $\Delta F/N$ versus d for systems with different R_l. For small $R_l = 10$, $\Delta F/N$ is always positive, but as R_l increases, the force drops below zero over a region that increases with increasing R_l, and returns to positive values at higher values of d. The resulting shape of $\Delta F/N(d)$ resembles an atomic interaction force curve, with a stable characteristic distance determined by the point at which $\Delta F/N$ crosses zero with positive slope, suggesting that freely moving walls could be stabilized at this spacing. These results show that by varying the geometry it is possible to achieve detailed control over the magnitude of the fluctuation-induced forces which could be useful for self-assembly.

C. Infinite walls

We have also considered the case of two infinite walls that confine the particles to an interior chamber, producing only an outward force. Such a system could be created by trapping bacteria or active particles in a confined geometry. We consider both one-dimensional (1D or linear) and 2D samples with different wall spacings d and constant particle density. For Brownian particles, $\Delta F/N$ is independent of d. In Fig. 5(a) we plot the outward force $-\Delta F/N$ versus d/R_l for a 1D system. When l is infinite, the only length scales are d and R_l. The fraction of time a particle spends traveling along the walls is unchanged if both these lengths are scaled by the same factor, so the force must be a function of d/R_l. In Fig. 5, the curves for various R_l collapse to the form $F(x) = 1/(1+x)$ with $x \equiv d/R_l$, which can be derived from elementary considerations.

For simplicity, let $x \equiv d/R_l$ be an integer, and measure length in units of R_l and time in units of τ. The particle moves in 1D along y with walls located at $y = 0$ and $y = x$. During each run time, the particle moves a distance ± 1 along y. To calculate the relative amount of time a particle spends at a wall, we note that a particle emerges into the bulk by tumbling away from a wall; taking this to be the $y = 0$ wall, the particle takes one step to $y = 1$. We then need to calculate the expected

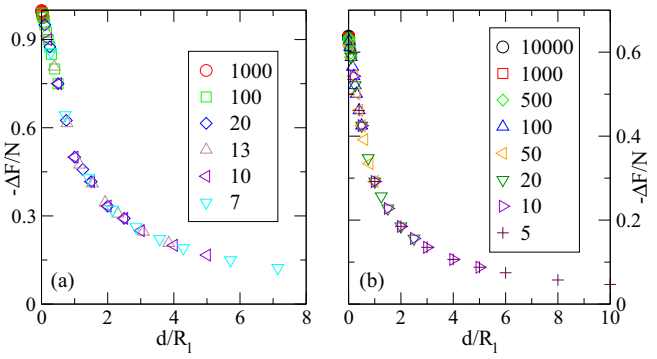

FIG. 5. (Color online) Outward force $-\Delta F/N$ vs d/R_l for particles confined between infinite walls at fixed particle density. (a) 1D systems with varied R_l (in legend) and d. The curves collapse to the functional form $\Delta F(d/R_l) = 1/(1 + d/R_l)$. (b) 2D systems with various d and R_l. The curves collapse to a similar functional form, with altered coefficients.

time t_b required for the particle to either return to $y = 0$ or reach $y = x$. This is the "gambler's ruin" problem, with the well-known solution [37] of $(x - 1)$. Counting the first step into the bulk, the expected number of steps in the bulk between wall motions is just x, so $t_b = x$. To determine t_w, the amount of time the particle spends at the wall after reaching it, we note that each tumble provides a 50:50 chance of escaping the wall, giving a probability $p = \frac{1}{2}$ that $t_w = 0$, $p = \frac{1}{4}$ that $t_w = 1$, and so on. The expected value of t_w is easily found to be $t_w = 1$. Therefore, the ratio of t_w to the total time is $t_w/(t_w + t_b) = 1/(1 + x)$. This equals the time-averaged force on the walls since in the 1D scenario, the force on a wall is 1 when a particle is present at the wall and 0 otherwise. For noninteger x, it is not too difficult to derive a more general formula $\frac{2-\frac{x}{\text{ceil}(x)}}{1+\text{ceil}(x)}$ where ceil(x) is the smallest integer $\geqslant x$.

In Fig. 5(b) we plot $-\Delta F/N$ for a 2D system. Here we could not derive a fully analytic solution; however, we obtain a fit of $F(x) = a/(1 + bx)$ with $a = 2/\pi$ and $b \approx 1.25$. The value for a is exact and arises because in 2D all angles of incidence are possible rather than just normal incidence. Since the angle distribution is uniform, the force on the wall decreases by a factor of $\frac{1}{\frac{\pi}{2}-0}\int_0^{\pi/2} \cos\theta\, d\theta = 2/\pi$. We cannot calculate b exactly, but it can be understood heuristically: Compared to the 1D derivation, the particle spends more time in the bulk because only the x component of its motion moves it towards a wall. This increases the number of steps required to reach a wall, giving $b > 1$.

When steric particle-particle interactions are included, the forces on the walls will be reduced; however, in the dilute limit these results should hold and should be readily testable in experiments. It would also be interesting to study forces between two spheres or a sphere and a wall. In this case it would be important to understand how particles move along curved surfaces [34].

IV. SUMMARY

We show that in a Casimir geometry of two parallel walls placed in a bath of run-and-tumble active particles, a robust attractive force arises between the walls due to a combination of particles moving along the walls and a geometric shadowing effect that depletes the particle density between the walls. The force increases when the depletion becomes more pronounced for increasing particle run length or reduced wall spacing. Our results are robust against the inclusion of steric particle-particle interactions in the dilute limit. For other geometries such as two walls containing small apertures, a particle trapping effect can produce repulsive forces between the walls. Our results show that active matter systems can exhibit a rich variety of fluctuation-induced forces between objects, which may be useful for applications such as self-assembly or particle transport.

Note added. Recently, we became aware of Ref. [38] on forces between two plates produced by active colloids with steric particle-particle interactions, where in the dilute limit a long-range attractive force arises of the same form that we observe. This indicates that our run-and-tumble results should also apply to active colloid systems. In the dense limit a repulsive force is caused by crystallization of the particles between the plates [38]. Additionally, Ref. [39] considers a Casimir type effect for swimming particles.

ACKNOWLEDGMENTS

We thank D. Dalvit, L. Lopatina, and S. Redner for useful discussions. This work was carried out under the auspices of the NNSA of the U.S. DOE at LANL under Contract No. DE-AC52-06NA25396.

[1] H. B. G. Casimir, Proc. K. Ned. Akad. Wet. **51**, 793 (1948).
[2] S. K. Lamoreaux, Phys. Rev. Lett. **78**, 5 (1997).
[3] F. Intravaia, S. Koev, I. W. Jung, A. A. Talin, P. S. Davids, R. S. Decca, V. A. Aksyuk, D. A. R. Dalvit, and D. Lopez, Nat. Commun. **4**, 3515 (2013).
[4] J. N. Munday, F. Capasso, and V. A. Parsegian, Nature (London) **457**, 170 (2009).
[5] M. E. Fisher and P. G. de Gennes, C. R. Acad. Sci., Ser. B **287**, 207 (1978).
[6] C. Hertlein, L. Helden, A. Gambassi, S. Dietrich, and C. Bechinger, Nature (London) **451**, 172 (2008).
[7] A. Hanke, F. Schlesener, E. Eisenriegler, and S. Dietrich, Phys. Rev. Lett. **81**, 1885 (1998); A. Gambassi, J. Phys.: Conf. Ser. **161**, 012037 (2009).
[8] D. Bonn, J. Otwinowski, S. Sacanna, H. Guo, G. Wegdam, and P. Schall, Phys. Rev. Lett. **103**, 156101 (2009); A. Gambassi and S. Dietrich, *ibid.* **105**, 059601 (2010).
[9] S. J. Veen, O. Antoniuk, B. Weber, M. A. C. Potenza, S. Mazzoni, P. Schall, and G. H. Wegdam, Phys. Rev. Lett. **109**, 248302 (2012); V. D. Nguyen, S. Faber, Z. Hu, G. H. Wegdam, and P. Schall, Nat. Commun. **4**, 1584 (2013).
[10] S. Buzzaccaro, J. Colombo, A. Parola, and R. Piazza, Phys. Rev. Lett. **105**, 198301 (2010).

[11] C. Cattuto, R. Brito, U. M. B. Marconi, F. Nori, and R. Soto, Phys. Rev. Lett. **96**, 178001 (2006); Y. Y. Villanueva, D. V. Denisov, S. de Man, and R. J. Wijngaarden, Phys. Rev. E **82**, 041303 (2010).
[12] N. Gnan, E. Zaccarelli, and F. Sciortino, Nat. Commun. **5**, 4267 (2014).
[13] B. B. Machta, S. L. Veatch, and J. P. Sethna, Phys. Rev. Lett. **109**, 138101 (2012).
[14] S. Ramaswamy, Annu. Rev. Condens. Matter Phys. **1**, 323 (2010); M. C. Marchetti, J. F. Joanny, S. Ramaswamy, T. B. Liverpool, J. Prost, M. Rao, and R. A. Simha, Rev. Mod. Phys. **85**, 1143 (2013).
[15] H. C. Berg, *Random Walks in Biology* (Princeton University Press, Princeton, 1983).
[16] P. Galajda, J. Keymer, P. Chaikin, and R. Austin, J. Bacteriol. **189**, 8704 (2007).
[17] R. Dreyfus, J. Baudry, M. L. Roper, M. Fermigier, H. A. Stone, and J. Bibette, Nature (London) **437**, 862 (2005).
[18] W. F. Paxton, K. C. Kistler, C. C. Olmeda, A. Sen, S. K. St. Angelo, Y. Y. Cao, T. E. Mallouk, P. E. Lammert, and V. H. Crespi, J. Am. Chem. Soc. **126**, 13424 (2004); J. R. Howse, R. A. L. Jones, A. J. Ryan, T. Gough, R. Vafabakhsh, and R. Golestanian, Phys. Rev. Lett. **99**, 048102 (2007); R. Golestanian, *ibid.* **102**, 188305 (2009).
[19] G. Volpe, I. Buttinoni, D. Vogt, H.-J. Kummerer, and C. Bechinger, Soft Matter **7**, 8810 (2011).
[20] J. Palacci, S. Sacanna, A. P. Steinberg, D. J. Pine, and P. M. Chaikin, Science **339**, 936 (2013).
[21] I. Buttinoni, J. Bialke, F. Kümmel, H. Löwen, C. Bechinger, and T. Speck, Phys. Rev. Lett. **110**, 238301 (2013).
[22] J. Tailleur and M. E. Cates, Phys. Rev. Lett. **100**, 218103 (2008); A. G. Thompson, J. Tailleur, M. E. Cates, and R. A. Blythe, J. Stat. Mech.: Theory Exp. (2011) P02029.
[23] J. Bialke, T. Speck, and H. Löwen, Phys. Rev. Lett. **108**, 168301 (2012).
[24] Y. Fily and M. C. Marchetti, Phys. Rev. Lett. **108**, 235702 (2012); G. S. Redner, M. F. Hagan, and A. Baskaran, *ibid.* **110**, 055701 (2013); C. Reichhardt and C. J. Olson Reichhardt, Phys. Rev. E **90**, 012701 (2014).
[25] M. E. Cates and J. Tailleur, Europhys. Lett. **101**, 20010 (2013).
[26] M. B. Wan, C. J. Olson Reichhardt, Z. Nussinov, and C. Reichhardt, Phys. Rev. Lett. **101**, 018102 (2008); C. Reichhardt and C. J. Olson Reichhardt, Phys. Rev. E **88**, 062310 (2013).
[27] J. Tailleur and M. E. Cates, Europhys. Lett. **86**, 60002 (2009).
[28] L. Angelani, A. Costanzo, and R. Di Leonardo, Europhys. Lett. **96**, 68002 (2011); V. Kantsler, J. Dunkel, M. Polin, and R. E. Goldstein, Proc. Natl. Acad. Sci. USA **110**, 1187 (2013); I. Berdakin, Y. Jeyaram, V. V. Moshchalkov, L. Venken, S. Dierckx, S. J. Vanderleyden, A. V. Silhanek, C. A. Condat, and V. I. Marconi, Phys. Rev. E **87**, 052702 (2013).
[29] M. E. Cates, Rep. Prog. Phys. **75**, 042601 (2012).
[30] L. Angelani, R. Di Leonardo, and G. Ruocco, Phys. Rev. Lett. **102**, 048104 (2009); R. Di Leonardo, L. Angelani, D. Dell'Arciprete, G. Ruocco, V. Iebba, S. Schippa, M. P. Conte, F. Mecarini, F. De Angelis, and E. Di Fabrizio, Proc. Natl. Acad. Sci. USA **107**, 9541 (2010).
[31] A. Sokolov, M. M. Apodaca, B. A. Grzybowski, and I. S. Aranson, Proc. Natl. Acad. Sci. USA **107**, 969 (2010).
[32] N. Koumakis, A. Lepore, C. Maggi, and R. Di Leonardo, Nat. Commun. **4**, 2588 (2013).
[33] L. Angelani and R. Di Leonardo, New J. Phys. **12**, 113017 (2010).
[34] Y. Fily, A. Baskaran, and M. F. Hagan, Soft Matter **10**, 5609 (2014).
[35] J. A. Drocco, C. J. Olson Reichhardt, and C. Reichhardt, Phys. Rev. E **85**, 056102 (2012).
[36] L. Angelani, C. Maggi, M. L. Bernardini, A. Rizzo, and R. Di Leonardo, Phys. Rev. Lett. **107**, 138302 (2011).
[37] S. Redner, *A Guide to First-Passage Processes* (Cambridge University Press, Cambridge, 2001).
[38] R. Ni, M. A. C. Stuart, and P. G. Bolhuis, arXiv:1403.1533.
[39] C. Parra-Rojas and R. Soto, Phys. Rev. E **87**, 053022 (2013).